Article

Point-of-Care Assay of Alkaline Phosphatase Enzymatic Activity Using Thermometer or Temperature Discoloration Sticker as Readout

Xiaofeng Liu, Liyuan Zou, Xiaohai Yang, Qing Wang, Yan Zheng, Xiuhua Geng, Guofu Liao, Wenyan Nie, and Kemin Wang

Anal. Chem., **Just Accepted Manuscript** • Publication Date (Web): 22 May 2019

Point-of-Care Assay of Alkaline Phosphatase Enzymatic Activity Using Thermometer or Temperature Discoloration Sticker as Readout

Xiaofeng Liu, Liyuan Zou, Xiaohai Yang, Qing Wang*, Yan Zheng, Xiuhua Geng, Guofu Liao, Wenyan Nie, Kemin Wang*

State Key Laboratory of Chemo/Biosensing and Chemometrics, College of Chemistry and Chemical Engineering, Key Laboratory for Bio-Nanotechnology and Molecular Engineering of Hunan Province, Hunan University, Changsha 410082, China.

* E-mail address: wwqq99@hnu.edu.cn, kmwang@hnu.edu.cn Tel/Fax: +86-731-88821566.

ABSTRACT: Alkaline phosphatase (ALP) is a significant biomarker in clinical diagnostics, and the abnormal level of ALP enzyme in serum is closely related to various diseases such as bone or liver cancer, bone metastases and extrahepatic biliary obstruction. Herein, a simple and portable photothermal biosensor was developed for sensitive detection of ALP enzyme based on the formation of polydopamine (PDA) nanoparticles using thermometer or temperature discoloration sticker as readout. MnO_2 nanosheet was firstly prepared using a novel one-pot strategy which showed operational simplicity and low time-consuming. Then dopamine (DA) was quickly polymerized into PDA nanoparticles in the presence of MnO_2 nanosheet. When the model analyst ALP was present, the substrate 2-phospho-L-ascorbic acid trisodium salt (AAP) was catalytically hydrolyzed into L-ascorbic acid (AA), resulting in the inhibition of the formation of the PDA nanoparticles owing to the fact that MnO_2 nanosheet was reduced into Mn^{2+} by generated AA. Thus, a portable biosensor based on the photothermal properties of PDA nanoparticles for ALP enzyme detection was established with a detection limit as low as 0.1 U/L (thermometer) and 1 U/L (temperature discoloration sticker). In addition, it also showed excellent sensing performance for the ALP assay in human serum. Such a simple, label-free, cost-effective, and sensitive assay could exhibit real potential application for ALP detection and early diagnosis in the world, especially in developing countries or remote regions.

Alkaline phosphatase (ALP) is an necessary hydrolase in human body, that could split the phosphate functional groups from a range of substrate molecules including nucleic acids, proteins etc. [1-3] In addition, ALP enzyme is also confirmed as significant biomarker in the diagnosis of various diseases, such as liver dysfunction and cancer, [4] leucocythemia, [5] Alzheimer's disease, [6] biliary obstruction [7] and bone metastasis from prostate carcinoma. [8] Therefore, developing the portable and sensitive biosensor for ALP detection will benefit the diagnoses of some diseases and biomedical research.

The colorimetric methods based on the generation of colored products catalyzed by ALP enzyme was widely used in clinical tests because of its simplicity and low cost. [9-13] Besides, other colorimetric methods were also developed for visual readout of ALP due to the local surface plasmon resonance (LSPR) of gold and silver nanoparticles. [14,15] However, the colorimetric methods remain some limits such as low sensitivity and easy interference. [16] To improve the detection sensitivity, a range of analytical methods have been developed for ALP detection such as fluorescence, [17-21] electrochemistry, [22] electrochemiluminescence, [23] surface enhancement Raman scattering (SERS)[24,25] and inductively coupled plasma mass spectrometry (ICP-MS). [26] Although these methods showed high sensitivity and precision, it was difficult to be utilized in the point of care (POC) detection due to the limited respects such as the expensive modification, vulnerable interference and large instrument and professional operator. [27, 28] Currently, few papers have focused on the simple, portable and low-cost method for POC detection of ALP. Thus, it is still highly desirable to develop more rational, direct, and sensitive methods for detecting ALP levels, especially using the commercially and easily available common devices.

The thermometer is one of the most common measurement in daily life, owing to its easy operation, low cost and short time-consuming etc. It has reported that some biomarkers could be measured using temperature as readout. [29-34] However, most of the methods were still limited in these aspects including low photothermal generation efficiency, complex entrapment and decoration steps of photothermal reagents, low signal-to-background ratio owing to the leakage of photothermal reagents and so on. Therefore, it is of great significance to develop a convenient and highly sensitive POC assay for quantitative and qualitive ALP analysis using temperature signals. Herein, taking advantages of the photothermal effect with polydopamine (PDA) nanoparticles, a very simple and portable biosensor based on the formation of PDA nanoparticles was developed for ALP enzyme detection using thermometer (quantitative analysis) or temperature discoloration sticker (qualitative analysis) as readout. The temperature discoloration sticker was composed of five thermochromic dyes (the temperature of discoloration was 31 ºC, 33 ºC, 35 ºC, 37 ºC and 41 ºC, respectively), and

then was coated on Ep tube wall. The thermochromic dye showed original color below the temperature of discoloration, while it gradually appeared achromatic color above the temperature of discoloration. As shown in Scheme 1, in the absence of ALP, PDA nanoparticles could be synthesized by the oxidization of dopamine with MnO_2 nanosheets, showing the strong photothermal efficiency. However, in the presence of ALP, 2-phospho-L-ascorbic acid trisodium salt (AAP), which was one of the most frequently used specific substrates in the ALP activity assays, [35-37] was transformed to L-ascorbic acid (AA). Subsequently, the generated AA could reduce MnO_2 to Mn^{2+} and it was also oxidized to dehydrogenated ascorbic acid (DHA) (Scheme S1). And the produced Mn^{2+} and DHA could not oxidize dopamine into PDA nanoparticles. PDA nanoparticles had the light-to-heat conversion under the NIR irradiations, resulting the temperature change of the solution. Thus, the concentration of ALP detection was facilely achieved based on the change values of temperature. With the concentration of ALP increasing, the temperature change raised greatly, and the temperature discoloration sticker changed from colorless to different color. This work may provide a new insight on the application of PDA nanoparticles to develop the facile and sensitive biosensor.

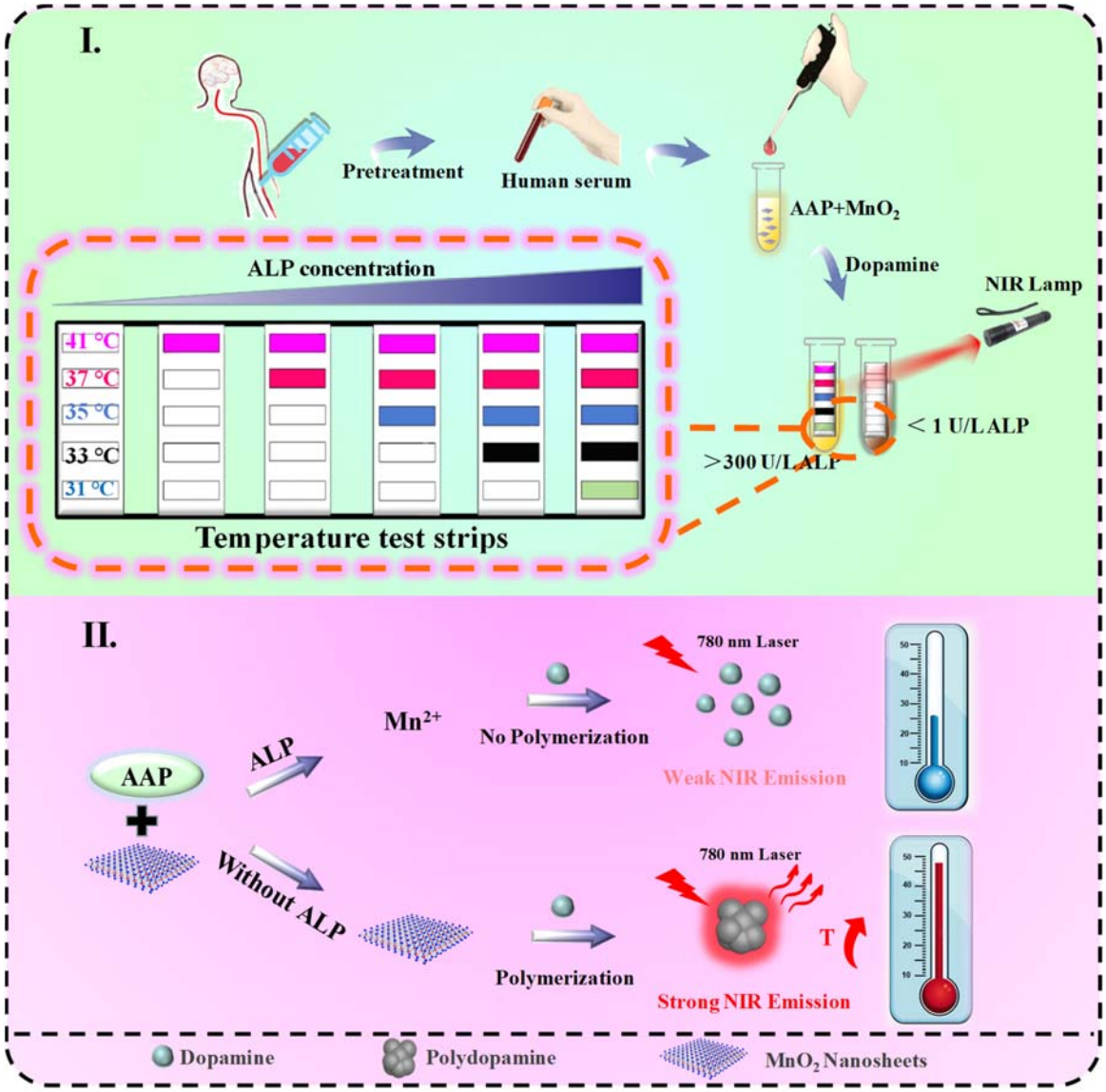

Scheme 1. Schematic illustration of rapid and portable photothermal biosensor for sensitive detection of ALP

EXPERIMENTAL SECTION

Materials and Reagents. 2-Phospho-L-ascorbic acid trisodium salt (AAP) and alkaline phosphatase (ALP) enzyme from bovine intestinal mucosa were obtained from Sigma-Aldrich (St. Louis, MO, U.S.A.). Dopamine and $KMnO_4$ were purchased from Sinopharm Chemical Reagent Co., Ltd (Shanghai, China). Polyvinyl pyrrolidone (PVP) was purchased by Sangon Biotech. Co., Ltd. (Shanghai, China). The human serum samples were collected from healthy volunteers. All the chemical reagents were of analytical grade and used without further purification. Ultrapure water (18.2 MΩ · cm) was used to prepare all reagents in the experiments. Five kind of thermochromic dyes and portable infrared laser (780 nm) were purchased from Taobao (China, website: http://www.taobao.com/).

Preparation and Characterization of MnO_2 Nanosheets. The redox method was used for synthesizing the MnO_2 nanosheets. In detail, 1.6 mM PVP solution (pH 3.0) was adjusted by sulfuric acid. The mixed solution was heated to 85 ºC for 15 minutes. Then, 0.5 mM $KMnO_4$ was added and incubated for 2 h at 85 ºC. Next, the mixture solution was centrifuged at 10,000 rpm for a quarter to purify MnO_2 nanosheets. The precipitate was washed three times with ethanol and ultrapure water, then dried in a vacuum freeze dryer. The characterization of MnO_2 nanosheets was acquired by JEM-2100Plus (JEOL, Japan). Dynamic light scattering (DLS) and Zeta potential of MnO_2 nanosheets were also performed using a Zeta-sizer Nano ZS90 (Malvern Instruments, UK).

Synthesis and Characterization of PDA Nanoparticles. An existing synthetic route was used for the synthesis of PDA nanoparticles. [38,39] 20 μg/mL MnO_2 nanosheets was added into 20 μg/mL dopamine solution. After incubating at room temperature for 30 min, PDA nanoparticles were formed. Next, the addition of 10 μL 0.1 M HCl was used for halting the polymerization reaction. The transmission electron microscopy (TEM) and energy dispersive X-ray spectroscopy (EDS) characterization of PDA nanoparticles was acquired by JEM-2100Plus (JEOL, Japan). DLS and Zeta potential of PDA nanoparticles were also performed using a Zeta-sizer Nano ZS90 (Malvern Instruments, UK).

Detection of ALP in Aqueous Buffer and Human Serum Samples. PDA nanoparticle-based assay for detection of ALP activity was investigated under the next procedures. For the ALP detection, 20 μg/mL MnO_2, 23 μg/mL AAP and different concentrations of ALP were incubated in Tris-HCl buffer (pH 7.4) at 30 ºC for 40 min. Then, 20 μg/mL dopamine was added. After being blended, the mixture was incubated at 25 ºC for 0.5 h. Next, 0.1 M HCl (20 μL) was added into the solution. Then, the reaction solution was irradiated using 780 nm laser for 10 min and the temperature change was monitored by thermometer or temperature discoloration sticker.

For avoiding protein interference, the serum samples were treated. Firstly, the trichloroacetic acid (quality fraction 15%) and N-ethylmaleimide (47.5 μg/mL) was added into 1 mL serum for deactivating the enzymes/proteins in the serum. After centrifuged for a quarter at 12 000 rpm, the supernatant was modulated to pH 7.4. Then, different concentrations of ALP were added into the treated serum samples and the spiked samples (30%) were obtained. Next, the ALP in the spiked samples were detected using the above-mentioned method.

RESULTS and DISCUSSION

Characterization of MnO_2 Nanosheets. MnO_2 nanosheets were synthesized using a one-pot method that $KMnO_4$ was reduced in PVP solution. Compared to the previous methods, [40-42] our proposed method has some obvious merits including the mild reaction conditions (no need for high pressure) and low time-consuming. The synthesized MnO_2 nanosheets was characterized using a series of techniques. As shown in Figure S1, compared to $KMnO_4$, MnO_2 nanosheets emerged a new absorption peak at 400 nm, which was consistent with previous reports.[32] TEM image in Figure 1A clearly showed typical nanosheet morphology of MnO_2 nanosheets. EDS measurement of the synthesized MnO_2 confirmed the presence of Mn and O elements with the atomic ratio of 1:2 (shown in Figure 1B). DLS measurement of MnO_2 nanosheets exhibited a hydrodynamic diameter of 206 ± 50 nm and the zeta potential of such nanosheets was -25 ± 5 mV (shown in Figure S2). The results indicated that MnO_2 nanosheets were successfully synthesized. In addition, such MnO_2 nanosheets had excellent dispersibility and were not agglomerated for three weeks.

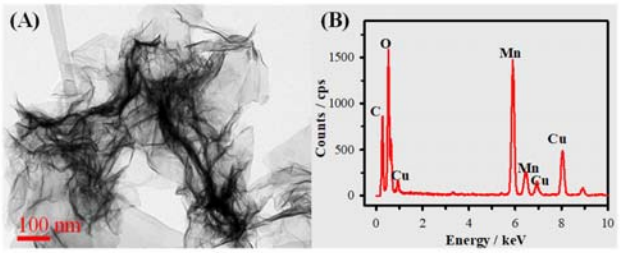

Figure 1. The characterization of MnO_2 nanosheets. (A) TEM image of the as-prepared MnO_2 nanosheets. Scale bar: 100 nm. (B) EDS spectrum of the synthesized MnO_2 nanosheets.

Characterization of PDA Nanoparticles. PDA nanoparticles were synthesized though oxidizing dopamine using MnO_2 nanosheets. The PDA nanoparticles were spherical in shape and well dispersed in water, and the sizes of PDA nanoparticles were mostly distributed in the range from 6 to 12 nm, with an average size of 9 nm (Figure 2A). In Figure 2B, the high-resolution TEM (HRTEM) images showed that PDA nanoparticles exhibited identically well-resolved lattice fringes with interplanar spacings of 0.23 nm.

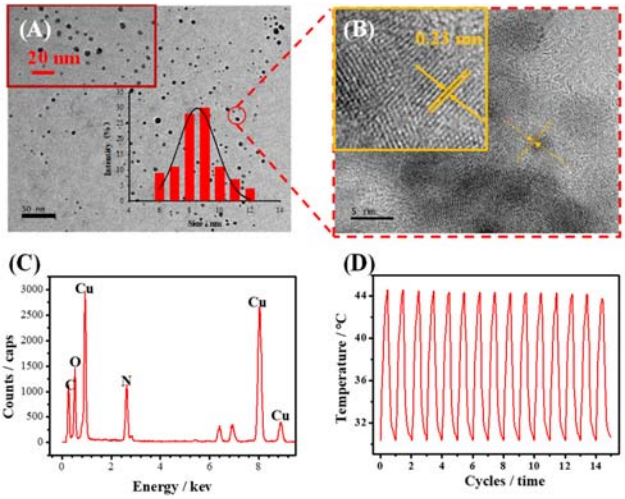

Figure 2. The characterization of PDA nanoparticles. (A) TEM image of the as-prepared MnO_2 nanosheets. Scale bar: 50 nm. (Insert: Size distribution of PDA nanoparticles in diameter measured by TEM). (B) High-resolution TEM image of PDA nanoparticle. (C) EDS spectrum of the synthesized PDA nanoparticles. (D) Photothermal stability experiment of PDA nanoparticles over multiple ON/OFF cycles in laser irradiation (780 nm, 0.7 W/cm^2).

As shown in Figure 2C, compositional analysis of PDA nanoparticles by EDS measurement showed the signals of C, N and O elements. The synthesized PDA nanoparticles were also characterized by UV-vis absorption spectroscopy, as shown in Figure S3. Compared to dopamine, PDA nanoparticles showed weak intense absorption value at 220 and 280 nm because of the formation of quinone units. And compared to MnO_2 nanosheets, the absorption peak of PDA nanoparticles at around 400 nm decreased significantly. In addition, PDA nanoparticles exhibited

a hydrous particle diameter distribution (15 ± 3nm) which were nearly to the TEM results and negative charge (-34 ± 10 mV) (shown in Figure S4). The results indicated that PDA nanoparticles were successfully synthesized.

Furthermore, as shown in Figure S5, the temperature of PDA nanoparticles rose obviously with the prolongation of NIR laser time, while the temperature of MnO_2 nanosheets or dopamine increased unobviously. The results illustrated that the PDA nanoparticles showed an excellent NIR laser-driven photothermal effect. Besides, the photostability of PDA nanoparticles was also tested. No obvious photobleaching of PDA nanoparticles was observed after exposure to a 780 nm laser for 15 cycle times (shown in Figure 2D). It illustrated that the PDA nanoparticles has excellent photothermal stability.

Investigation of the Feasibility. The feasibility was investigated (shown in Figure 3). Compared to the absence of ALP enzyme (black dots), the temperature change values after the NIR laser irradiation decreased when ALP enzyme was added to the reaction system (purple triangles) (shown in Figure 3A). Evidently, when ALP was added into the reaction solution, it could catalyze AAP to AA. Subsequently, the generated AA could reduce MnO_2 to Mn^{2+}. Since the produced Mn^{2+} could not oxidize dopamine into PDA nanoparticles, showing weak photothermal efficiency. Furthermore, the feasibility was also studied by temperature discoloration sticker as the readout. The photograph and infrared image of the reaction system with or without ALP were shown in Figure 3B. In the absence of ALP, both the photograph and infrared image of the reaction system showed the dramatic color change after laser irradiation. Conversely, no obvious color change was displayed after laser irradiation when ALP was present. The above results demonstrated the feasibility of the proposed assay.

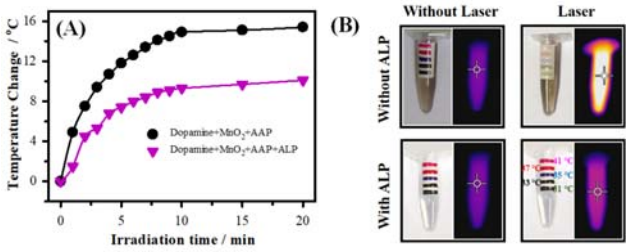

Figure 3. The investigation of the feasibility of the proposed biosensor. (A) Temperature change value in laser irradiation (780 nm, 0.7 W/cm^2) of different circumstances. (B) The photograph and infrared image of the reaction system with or without ALP and laser.

ALP Detection Using Thermometer. To optimize the performance of the biosensor, the effect of some parameters (including the concentration of MnO_2 nanosheets and dopamine, buffer solution, Mg^{2+} concentration, the reaction time) was investigated by photothermal assay. The results (in Figure S6) showed that 20 μg/mL were selected as the optimal concentration of MnO_2 nanosheets and dopamine, respectively. Besides, 10 mM Tris-HCl buffer (pH 7.4), the reaction time for 40 min among ALP, AAP and MnO_2 nanosheets, Mg^{2+} concentration (5 mM), the power density (0.7 W/cm^2) and irradiation time (10 min) of 780 nm NIR lamp were chosen as the optimal conditions (as shown in Figure S7).

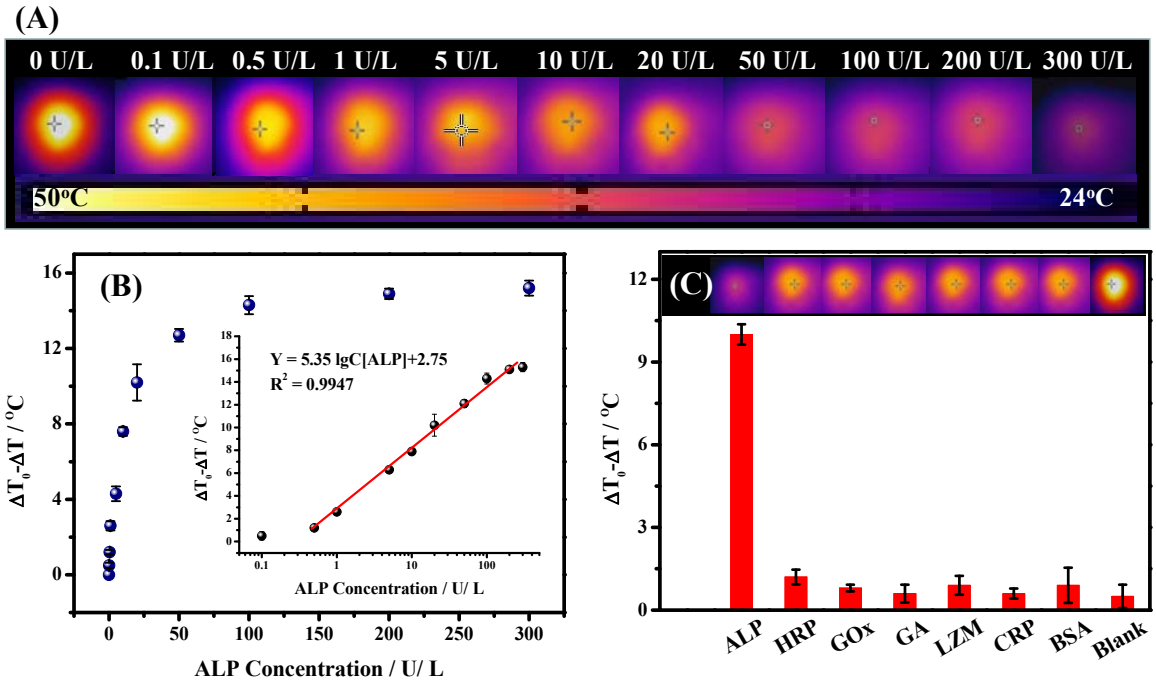

Figure 4. (A) The infrared image of PDA nanoparticles during 10 min of laser irradiation (780 nm, 0.7 W / cm^2) in the presence of different concentrations of ALP, ranging from 0.0 to 300.0 U/L, (B) Relationship between temperature change values (ΔT_0 - ΔT) and the ALP concentration, (C) Selectivity investigation of the proposed biosensor. The concentration of these proteins was 2 mg/mL. Error bars were standard deviation of three repetitive experiments. (ΔT_0 was the temperature change values in the absence of ALP enzyme, and ΔT was the temperature change value in the presence of ALP enzyme).

Then, ALP detection was investigated using photothermal assay platform based on the PDA nanoparticles with a thermometer under the optimal experimental conditions. As shown in Figure 4A, the intensity value of infrared imaging with PDA nanoparticles was gradually decreased as the increase of ALP concentration in the range from 0.0 to 300.0 U/L. It displayed an excellent linear relationship between the temperature change values ($\Delta T_0 - \Delta T$) and the logarithm of ALP level with concentrations of 0.5 U/L to 200.0 U/L (Figure 4B). ΔT_0 was defined as the temperature change after the NIR laser irradiation in the absence of ALP enzyme. ΔT was defined as the temperature change after the NIR laser irradiation in the presence of ALP enzyme. The method covered the range of clinical useful values of ALP concentration (50-135 U/L for the female; 45-125 U/L for the male), [43] implying that it could be used in clinical detection of ALP enzyme. When the concentration of ALP enzyme was 0.1 U/L, it was measured that the ($\Delta T_0 - \Delta T$) was 0.6 using thermometer, which was greater than 3σ value ($\sigma = 0.14$). However, as 0.05 U/L ALP enzyme was detected, the ($\Delta T_0 - \Delta T$) was 0.1, which was lower than 3σ value. Therefore, the detection limit (LOD) for ALP detection was estimated to be 0.1 U/L using thermometer as readout, which was equal to or better than the previous methods for ALP enzyme detection. (Table S1)

To evaluate the selectivity of the proposed assay, the effect of several enzymes/proteins, including horseradish peroxidase (HRP), glucose oxidase (Gox), glucoamylase (GA), lysozyme (LZM), C-reactive protein (CRP) and bovine serum albumin (BSA) was investigated. As shown in Figure 4C, compare to blank sample, the temperature change values ($\Delta T_0 - \Delta T$) had no significant change after adding other enzymes/proteins, while a dramatic $\Delta T_0 - \Delta T$ increasing was showed in the presence of ALP. It demonstrated that the other proteins have negligible effect on the temperature change values of the PDA nanoparticle, suggesting that the biosensor had excellent selectivity towards ALP enzyme.

Table 1 Detection of ALP enzyme in human serum sample based on photothermal assay.

Serum samples	Added ALP (U/L)	Found ALP (U/L)	Recovery (%)	RSD (n = 3, %)
1	1	1.0	100	3.3
2	10	9.9	99.0	2.2
3	50	51.3	102.6	5.1
4	100	98.6	98.6	4.3

In addition, the developed PDA photothermal biosensor was also tested for ALP enzyme detection in human serum samples. The serum samples were regarded as having no ALP enzyme due to eliminating any protein interference through trichloroacetic acid. In addition, the ALP enzyme in serum samples was also investigated using the standard addition method. As shown in Table 1, the recoveries of ALP in serum sample varied from 98.6% to 102.6%, and the relative standard deviation (RSD) was from 2.2% to 5.1%. The results indicated that the method had potential applications for ALP enzyme detection in real samples. Given that ambient temperature was one of the most non-negligible elements when the temperature was acted as readout signals, the effect of ambient temperature was investigated. The results demonstrated that the POC assay was little affected by the ambient temperature in interior temperature (20 ºC to 30 ºC) (shown in Figure S8).

ALP Detection Using Temperature Discoloration Sticker. Given the convenience of color changes in POCT, the proposed assay was also demonstrated using temperature discoloration sticker as readout. The temperature discoloration sticker was composed of different thermochromic dyes, and then was coated on Ep tube. These thermochromic dyes on Ep tube displayed its original color below the temperature of discoloration. As it was above the temperature of discoloration, the achromatic color was appeared. Here, the temperature discoloration sticker showed pink (41 ºC), red (37 ºC), blue (35 ºC), black (33 ºC) and green (31 ºC) strips. After a series of ALP solution with concentrations ranging from 0.0 to 200.0 U/L were added into the reaction system and then was irradiated using 780 nm laser for 10 min, the color change of the temperature discoloration sticker was monitored. The results showed that the green, black, blue, red and pink strip gradually appeared from white with the increase of ALP concentrations. In addition, after laser irradiation, the intensity value of infrared imaging was gradually decreased as the increase of ALP concentration (Figure 5).

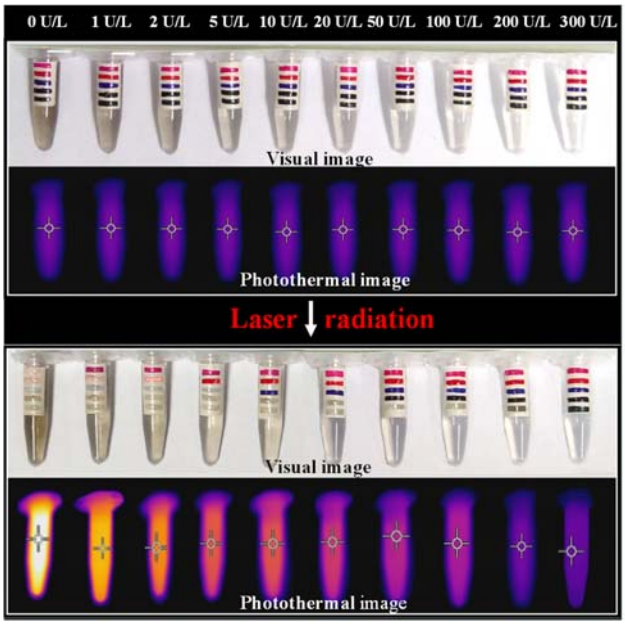

Figure 5. The visual and infrared images of different concentrations of ALP ranging from 0.0 to 200.0 U/L before and after laser irradiation (780 nm, 0.7 W/cm^2). The color of strips from top to bottom were pink (41 ºC), red (37 ºC), blue (35 ºC), black (33 ºC) and green (31 ºC), respectively.

When the temperature discoloration sticker was used for the readout, the color change could be observed for the detection of 1 U/L ALP. While no obvious color change could be observed for the detection of 0.5 U/L ALP. Thus, the LOD for ALP detection was estimated to be 1 U/L using temperature discoloration sticker as readout. More importantly, the temperature discoloration sticker in Ep tube could also exhibit a distinguishable color change by naked eye in low ALP concentration (1.0 U/L), of which was equal to and even better than that of the previous papers for ALP enzyme detection using colorimetric method. Similarly, it covered the range of clinical useful values of ALP concentration, [43] implying that the test strip could be used in clinical detection of ALP. In theory, the detection range and the LOD could be adjusted by changing the different thermochromic dyes.

To demonstrate the selectivity of the proposed assay, the effect of several proteins was also investigated (shown in Figure 6). The temperature discoloration sticker demonstrated five different colors as the ALP was present. Nevertheless, only one color was obviously observed in the presence of HRP, Gox, GA, LZM, CRP and BSA, respectively, which was similar to the blank sample. It demonstrated that the other proteins have negligible effect on the assay, implying that the biosensor had excellent selectivity towards ALP. In addition, different concentrations of ALP in the human serum samples, which were treated using the above-mentioned processing steps, were also tested. The results showed that ALP concentration in the human serum sample could be detected in the range of 1.0-100.0 U/L (shown in Figure S9). As the concentration of ALP enzyme increasing, the different color strip in the temperature discoloration sticker gradually appeared, suggesting that the assay showed the excellent performance in human serum. The results demonstrated that the proposed assay could be used for simple and visual detection of ALP enzyme.

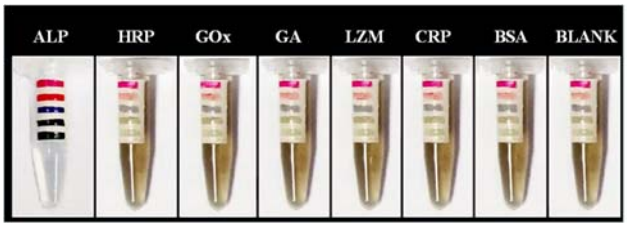

Figure 6. Selectivity investigation of the proposed biosensor. The visual image of the reaction solution during 10 min of laser irradiation in the presence of different protein. The concentration of these proteins was 2 mg/mL. The color of strips from top to bottom were pink (41 ºC), red (37 ºC), blue (35 ºC), black (33 ºC) and green (31 ºC), respectively.

CONCLUSIONS

In conclusion, a simple and portable photothermal biosensor was developed based on the formation of PDA nanoparticles for sensitive detection of ALP enzyme. The developed method showed some merits including simplicity, cost-effective, excellent selectivity and sensitivity. The detection limit of the biosensor was 0.1 U/L by thermometer. Even as low as 1 U/L ALP enzyme could be detected by temperature discoloration sticker, which covered the range of clinical useful values of ALP concentration. Furthermore, the proposed approach also showed excellent sensing performance for the detection of ALP in human serum. The biosensor based on photothermal effects of PDA nanoparticles could be extended for POC detection of other targets. This strategy may not only provide a new avenue for biomolecules sensing in biological application detection, but also be beneficial to the development of POC devices.

ASSOCIATED CONTENT

Supporting Information

The Supporting Information is available free of charge on the ACS Publications website.

Catalytic reaction equation of ALP enzyme, characterization of MnO_2 Nanosheets, characterization of PDA Nanoparticles, optimizations of experimental conditions, and ALP detection in human serum sample and comparison of analytical performance of some assays for ALP enzyme detection (PDF).

AUTHOR INFORMATION

Corresponding Author

E-mail: wwqq99@hnu.edu.cn. Tel./Fax: +86-731-8882 1566
E-mail: kmwang@hnu.edu.cn. Tel./Fax: +86-731-8882 1566

Author Contributions

The manuscript was written through contributions of all authors. / All authors have given approval to the final version of the manuscript.

Notes

The authors declare no competing financial interest.

ACKNOWLEDGMENT

This work was supported by the National Natural Science Foundation of China (21675047, 21375034 and 21735002), and National Science Foundation for Distinguished Young Scholars of Hunan Province (2016JJ1008).

REFERENCES

(1) Zheng, Z.; Chen, P.; Xie, M.; Wu, C.; Luo, Y.; Wang, W.; Jian g, J.; Liang, G. Cell Environment-Differentiated Self-Assembly of Nanofibers. *J. Am. Chem. Soc.* **2016**, *138*, 11128-11131.

(2) Zheng, F.; Guo, S.; Zeng, F.; Li, J.; Wu, S. Ratiometric Fluore scent Probe for Alkaline Phosphatase Based on Betaine-Modified Polyethylenimine via Excimer/Monomer Conversion. *Anal. Chem.* **2014**, *86*, 9873-9879.

(3) Wang, Z.; Sun, N.; He, Y.; Liu, Y.; Li, J. DNA Assembled Gol d Nanoparticles Polymeric Network Blocks Modular Highly Sensi tive Electrochemical Biosensors for Protein Kinase Activity Analy sis and Inhibition. *Anal. Chem.* **2014**, *86*, 6153-6159.

(4) Fernandez, N. J. Kidney, B. A. Alkaline Phosphatase: beyond The Liver. *Vet. Clin. Pathol.* **2007**, *36*, 223-233.

(5) Randolph, T. R. Chronic Myelocytic Leukemia-Part I: History, Clinical Presentation, and Molecular Biology. *Clin. Lab. Sci.* **200 5**, *18*, 38.

(6) Dong, L.; Qian, J.; Hai, Z.; Xu, J.; Du, W.; Zhong, K.; Liang, G. Alkaline Phosphatase-Instructed Self-Assembly of Gadolinium Nanofibers for Enhanced T_2-Weighted Magnetic Resonance Imag ing of Tumor. *Anal. Chem.* **2017**, *89*, 6922-6925.

(7) Taswell, H. F.; Jeffers, D. M. Isoenzymes of Serum Alkaline P hosphatase in Hepatobiliary and Skeletal Disease. *Am. J. Clin. Pat hol.* **1963**, *40*, 349-356.

(8) Wolf, P. L. Clinical Significance of Serum High-Molecular-Mass Alkaline Phosphatase, Alkaline Phosphatase-Lipoprotein-X Complex, and Intestinal Variant Alkaline Phosphatase. *J. Clin. Lab. Anal.* **1994**, *8*,172-176.
(9) Lei, L. L.; Xie, W. Y.; Chen, Z. Y.; Jiang, Y.; Liu, Y. S. Metal Ion Chelation-Based Color Generation for Alkaline Phosphatase-Linked High-Performance Visual Immunoassays. *Sens. Actuators B. Chem.* **2018**, *273*, 35-40.
(10) Lu, H. F.; Zhang, M. M.; Wu, D.; Huang, J. L.; Zhu, L. L.; Wang, C. M.; Zhang, Q. L. Colorimetric and Fluorescent Dual-Mode Sensing of Alkaline Phosphatase Activity in L-02 Cells and Its Application in Living Cell Imaging Based on In-Situ Growth of Silver Nanoparticles on Graphene Quantum Dots. *Sens. Actuators B. Chem.* **2018**, *258*, 461-469.
(11) Song, H. W.; Wang, H. Y.; Li, X.; Peng, Y. X.; Pan, J. M.; Niu, X. H. Sensitive and Selective Colorimetric Detection of Alkaline Phosphatase Activity Based on Phosphate Anion-Quenched Oxidase-Mimicking Activity of Ce (IV) Ions. *Anal. Chim. Acta.* **2018**, *1044*, 154-161.
(12) Guo, Y.; Wu, J.; Li, J.; Ju, H. A Plasmonic Colorimetric Strategy for Biosensing through Enzyme Guided Growth of Silver Nanoparticles on Gold Nanostars. *Biosens. Bioelectron.* **2016,** *78*, 267-73.
(13) Liu, T.; Li, N.; Dong, J. X.; Zhang, Y.; Fan, Y. Z.; Lin, S. M.; Luo, H. Q.; Li, N. B. A Colorimetric and Fluorometric Dual-Signal Sensor for Arginine Detection by Inhibiting The Growth of Gold Nanoparticles/Carbon Quantum Dots Composite. *Biosens. Bioelectron.* **2017**, *87*, 772-778.
(14) Jiao, H. Chen, J.; Li, W.; Wang, F.; Zhou, H.; Li, Y.; Yu, C. Nucleic Acid-Regulated Perylene Probe-Induced Gold Nanoparticle Aggregation: A New Strategy for Colorimetric Sensing of Alkaline Phosphatase Activity and Inhibitor Screening. *ACS. Appl. Mater. Interfaces* **2014**, *6*, 1979-1985.
(15) Gao, Z.; Deng, K.; Wang, X. D.; Miro, M.; Tang, D. High-Resolution Colorimetric Assay for Rapid Visual Readout of Phosphatase Activity Based on Gold/Silver Core/Shell Nanorod. *ACS. Appl. Mater. Interfaces* **2014**, *6*, 18243-18250.
(16) Hu, X. L.; Wu, X. M.; Fang, X.; Li, Z. J.; Wang, G. L. Switchable Fluorescence of Gold Nanoclusters for Probing The Activity of Alkaline Phosphatase and Its Application in Immunoassay. *Biosens. Bioelectron.* **2016**, *77*, 666-672.
(17) Chen, L.; Yang, G.; Wu, P.; Cai, C. Real-Time Fluorescence Assay of Alkaline Phosphatase in Living Cells Using Boron-Doped Graphene Quantum Dots as Fluorophores. *Biosens. Bioelectron.* **2017**, *96*, 294-299.
(18) Qian, Z.; Chai, L.; Tang, C.; Huang, Y.; Chen, J.; Feng, H. Carbon Quantum Dots-Based Recyclable Real-Time Fluorescence Assay for Alkaline Phosphatase with Adenosine Triphosphate as Substrate. *Anal. Chem.* **2015**, *87*, 2966-2973.
(19) Li, G.; Fu, H.; Chen, X.; Gong, P.; Chen, G.; Xia, L.; Wang, H.; You, J.; Wu, Y. Facile and Sensitive Fluorescence Sensing of Alkaline Phosphatase Activity with Photoluminescent Carbon Dots Based on Inner Filter Effect. *Anal. Chem.* **2016**, *88*, 2720-2726.
(20) Hai, Z.; Li, J.; Wu, J.; Xu, J.; Liang, G. Alkaline Phosphatase-Triggered Simultaneous Hydrogelation and Chemiluminescence. *J. Am. Chem. Soc.* **2017**, *139*, 1041-1044.
(21) Li, J.; Si, L.; Bao, J.; Wang, Z.; Dai, Z. Fluorescence Regulation of Poly(thymine)-Templated Copper Nanoparticles via an Enzyme-Triggered Reaction toward Sensitive and Selective Detection of Alkaline Phosphatase. *Anal. Chem.* **2017**, *89*, 3681-3686.
(22) Liu, C.; Dong, J.; Waterhouse, G. I. N.; Cheng, Z. Q.; Ai, S. Y. Electrochemical Immunosensor with Nanocellulose-Au Composite Assisted Multiple Signal Amplification for Detection of Avian Leukosis Virus Subgroup J. *Biosens. Bioelectron.* **2018**, *101*, 110-115.
(23) Jiang, H.; Wang, X. Alkaline Phosphatase-Responsive Anodic Electrochemiluminescence of CdSe Nanoparticles. *Anal. Chem.* **2012**, *84*, 6986-6993.
(24) Ingram, A.; Moore, B. D.; Graham, D. Simultaneous Detection of Alkaline Phosphatase and β-galactosidase Activity Using SERRS. *Bioorg. Med. Chem. Lett.* **2009**, *19*, 1569-1571.
(25) Bozkurt, A. G.; Buyukgoz, G. G.; Soforoglu, M.; Tamer, U.; Suludere, Z.; Boyaci, I. H. Alkaline Phosphatase Labeled SERS Active Sandwich Immunoassay for Detection of Escherichia Coli. *Spectrochim. Acta. A Mol. Biomol. Spectrosc.* **2018**, *194*, 8-13.
(26) Hasegawa, T.; Masaru, S.; Kohei, T.; Hirotaka, M.; Tomonari, U.; Hiroki, H. Assay of Alkaline Phosphatase in Salmon Egg Cell Cytoplasm with Fluorescence Detection of Enzymatic Activity and Zinc Detection by ICP-MS in Relation to Metallomics Research. *Bull. Chem. Soc. Jpn.* **2006**, *79*, 1211-1214;
(27) Lee, C. Y. Park, K. S. Park, H. G. A simple, Sensitive, and Label-Free Assay for Alkaline Phosphatase Activity Based on Target-Promoted Exponential Strand Displacement Amplification. *Sens. Actuators B. Chem.* **2018**, *262*, 1001-1005.
(28) Yang, L.; Li, J.; Pan, W.; Wang, H.; Li, N.; Tang, B. Fluorescence and Photoacoustic Dual-Mode Imaging of Tumor-Related MRNA with A Covalent Linkage-Based DNA Nanoprobe. *Chem. Commun.* **2018**, *54*, 3656-3659.
(29) Yakovleva, M.; Buzas, O.; Matsumura, H.; Samejima, M.; Igarashi, K.; Larsson, P. O.; Gorton, L.; Danielsson, B. A Novel Combined Thermometric and Amperometric Biosensor for Lactose Determination Based on Immobilised Cellobiose Dehydrogenase. *Biosens. Bioelectron.* **2012**, *31*, 251-256.
(30) Zhou, S. Zhao, Y. Mecklenburg, M.; Yang, D.; Xie, B. A Novel Thermometric Biosensor for Fast Surveillance of β-Lactamase Activity in Milk. *Biosens. Bioelectron.* **2013**, *49*, 99-104.
(31) Fu, G. L.; Sanjay, S. T.; Dou, M. W.; Li, X. J. Nanoparticle-Mediated Photothermal Effect Enables A New Method for Quantitative Biochemical Analysis Using A Thermometer. *Nanoscale* **2016**, *8*, 5422-5427.
(32) Fu, G.; Sanjay, S. T.; Zhou, W.; Brekken, R. A.; Kirken, R. A.; Li, X. Exploration of Nanoparticle-Mediated Photothermal Effect of TMB-H_2O_2 Colorimetric System and Its Application in a Visual Quantitative Photothermal Immunoassay. *Anal. Chem.* **2018**, *90*, 5930-5937.
(33) Zhang, J. Xing, H.; Lu, Y. Translating Molecular Detections into A Simple Temperature Test Using A Target-Responsive Smart Thermometer. *Chem. Sci.* **2018**, *9*, 3906-3910;
(34) Li, X.; Yang, L.; Men, C.; Xie, Y. F.; Liu, J. J.; Zou, H. Y.; Li, Y. F.; Zhan, L.; Huang, C. Z. Photothermal Soft Nanoballs Developed by Loading Plasmonic $Cu_{2-x}Se$ Nanocrystals into Liposomes for Photothermal Immunoassay of Aflatoxin B1. *Anal. Chem.* **2019**, *91*, 4444-4450.
(35) Xianyu, Y.; Wang, Z.; Jiang, X. A Plasmonic Nanosensor for Immunoassay via Enzyme-Triggered Click Chemistry. ACS Nano 2014, 8, 12741-12747.
(36) Sun, J.; Hu, T.; Chen, C.; Zhao, D.; Yang, F.; Yang, X. Fluorescence Immunoassay System via Enzyme-Enabled in Situ Synthesis of Fluorescent Silicon Nanoparticles. Anal. Chem. 2016, 88, 9789-9795.
(37) Zhao, D.; Li, J.; Peng, C.; Zhu, S.; Sun, J.; Yang, X. Fluorescence Immunoassay Based on the Alkaline Phosphatase Triggered in Situ Fluorogenic Reaction of o-Phenylenediamine and Ascorbic Acid. Anal. Chem. 2019, 91, 2978-2984.
(38) Xiao, T.; Sun, J.; Zhao, J.; Wang, S.; Liu, G.; Yang, X. FRET Effect between Fluorescent Polydopamine Nanoparticles and MnO_2 Nanosheets and Its Application for Sensitive Sensing of Alkaline Phosphatase. ACS. Appl. Mater. Interfaces **2018**, *10*, 6560-6569.
(39) Kong, X. J.; Wu, S.; Chen, T. T.; Yu, R. Q.; Chu, X. MnO_2-Induced Synthesis of Fluorescent Polydopamine Nanoparticles for

Reduced Glutathione Sensing in Human Whole Blood. Nanoscale **2016**, *8*, 15604-15610.
(40) Zhu, J.; He, J. Facile Synthesis of Graphene-Wrapped Honeycomb MnO_2 Nanospheres and Their Application in Supercapacitors. *ACS Appl. Mater. Interfaces* **2012,** *4*, 1770-1776.
(41) Deng, R.; Xie, X.; Vendrell, M.; Chang, Y. T.; Liu, X. Intracellular Glutathione Detection Using MnO_2-Nanosheet-Modified Upconversion Nanoparticles. *J. Am. Chem. Soc.* **2011,** *133*, 20168-20171.
(42) He, D. G.; He, X. X.; Wang, K. M.; Yang, X.; Yang, X.; Li, X.; Zou, Z. Nanometer-Sized Manganese Oxide-Quenched Fluorescent Oligonucleotides: An Effective Sensing Platform for Probing Biomolecular Interactions. *Chem. Commun.* **2014,** *50*, 11049-11052.
(43) Moss, D. W.; Whitby, L. G. A Simplified Heat-Inactivation Method for Investigating Alkaline Phosphatase Isoenzymes in Serum. *Clin. Chim. Acta*, **1975**, *61*, 63-71.

For TOC only: